Available online at www.sciencedirect.com

SCIENCE DIRECT

Developmental Biology 284 (2005) 364 – 376

DEVELOPMENTAL BIOLOGY

www.elsevier.com/locate/ydbio

A unique role for 6-*O* sulfation modification in zebrafish vascular development

Eleanor Chen[a,1], Sally E. Stringer[b,1,2], Melissa A. Rusch[b], Scott B. Selleck[b,*], Stephen C. Ekker[a,*]

[a]*Arnold and Mabel Beckman Center for Transposon Research, Department of Genetics, Cell Biology and Development, University of Minnesota, 6-160 Jackson Hall, 321 Church Street SE, Minneapolis, MN 55455, USA*

[b]*Developmental Biology Center, Departments of Pediatrics and Genetics, Cell Biology and Development, University of Minnesota, 6-160 Jackson Hall, 321 Church Street SE, Minneapolis, MN 55455, USA*

Received for publication 2 July 2004, revised 22 May 2005, accepted 25 May 2005
Available online 11 July 2005

Abstract

Heparan sulfate proteoglycans are important modulators of growth factor signaling in a variety of patterning processes. Secreted growth factors that play critical roles in angiogenesis bind to heparan sulfate, and this association is affected by 6-*O*-sulfation of the heparan sulfate chains. Addition of 6-*O*-sulfate is catalyzed by a family of sulfotransferases (HS6STs), and genetic manipulation of their function permits an assessment of their contribution to vascular assembly. We report on the biochemical activity and expression patterns of two zebrafish HS6ST genes. In situ hybridization reveals dynamic and distinct expression patterns of these two genes during development. Structural analysis of heparan sulfate from wild-type and morpholino antisense 'knockdown' embryos suggests that HS6ST-1 and HS6ST-2 have similar biochemical activity. HS6ST-2, but not HS6ST-1, morphants exhibit abnormalities in the branching morphogenesis of the caudal vein during embryonic development of the zebrafish. Our finding that HS6ST-2 is required for the branching morphogenesis of the caudal vein is the first in vivo evidence for an essential role of a gene encoding a heparan sulfate modifying enzyme in vertebrate angiogenesis. Our analysis of two zebrafish HS6ST genes suggests that a wide range of biological processes may be regulated by an array of sulfation-modifying enzymes in the vertebrate genome.

Keywords: Heparan sulfate 6-*O* sulfotransferase; Zebrafish; Vascular development; Morpholino

Introduction

Heparan sulfate proteoglycans (HSPGs) are present on the cell surface and in the extracellular matrix and play important roles in a variety of biological processes such as cell adhesion, wound healing and microbial pathogenesis (Rosenberg et al., 1997; Bernfield et al., 1999; Rapraeger, 2001). Each heparan sulfate chain attached to the protein core of an HSPG is composed of alternating D-glucuronic acid (GlcA) and *N*-acetyl-D-glucosamine units. *N*-sulfation of a proportion of the disaccharides occurs in blocks often referred to as S-domains. Within the S-domains other modifications take place, such as epimerization of GlcA to L-iduronic acid, sulfation at the 2-*O* position of uronic acid, or the 3-*O* position and the 6-*O* position of glucosamine. The sulfation pattern within the S-domains, as well as their length and spacing, contribute to the structural heterogeneity of heparan sulfate and may create specific binding sites for protein ligands (Esko and Selleck, 2002).

* Corresponding authors. S.B. Selleck is to be contacted at fax: +1 612 626 5652. S. C. Ekker, fax: +1 612 626 7031.
E-mail addresses: selle011@umn.edu (S.B. Selleck), ekker001@mail.med.umn.edu (S.C. Ekker).
[1] These authors contributed equally.
[2] Current address: School of Medicine, University of Manchester, Stopford Building, Oxford Road, Manchester, M13 9PT, UK.

0012-1606/$ - see front matter © 2005 Elsevier Inc. All rights reserved.
doi:10.1016/j.ydbio.2005.05.032

The interaction of heparan sulfate with protein ligands is often essential for modulating ligand-receptor binding and can influence the outcome of downstream signaling events (Perrimon and Bernfield, 2000; Esko and Selleck, 2002; Nakato and Kimata, 2002). The developmental abnormalities found in mutants deficient in the function of heparan sulfate biosynthetic enzymes have demonstrated the importance of heparan sulfate fine structure in regulating a variety of patterning and morphogenetic events in many organisms. For example, mice homozygous for a gene trap mutation in *Hs2st* show renal agenesis, eye and skeletal defects (Bullock et al., 1998). RNA interference of the *Drosophila* HS6ST gene produces defective branching in the tracheal system, a developmental system that shares many of the signaling components required for vertebrate angiogenesis (Kamimura et al., 2001).

In vitro studies have implicated heparan sulfate 6-*O* sulfation as a critical regulatory step in vessel formation. For example, 6-*O* desulfated heparin abolishes the amplifying effect of heparin on FGF-2 activation of FGFR-1 signaling and also inhibits FGF-2 induced angiogenesis (Lundin et al., 2000). The specific arrangement of 6-*O*-sulfated disaccharide units within heparan sulfate plays an important role in the binding of Endostatin, a peptide inhibitor of angiogenesis that requires heparan sulfate for its anti-angiogenic effect (Blackhall et al., 2003). While these in vitro studies suggest an important role for 6-*O* modification of heparan sulfate in vascular assembly, the functional requirement for this structural modification of HS in vivo is not known. We are using the zebrafish as a vertebrate model system to address the role of 6-*O* sulfation in vascular development, a highly conserved vertebrate developmental process (Roman and Weinstein, 2000; Weinstein, 2002). In contrast to mammals, passive diffusion of oxygen can sustain survival of zebrafish embryos without functional vasculature. This advantage permits the identification of genes essential for different stages of vascular development.

In this study, we have examined the function and expression of two zebrafish heparan sulfate 6-*O* sulfotransferase (HS6ST) genes, HS6ST-1 and HS6ST-2. The HS6ST-2 gene was originally identified from a morpholino-based screen for genes affecting vascular assembly and function in zebrafish, and its role in muscle development has been previously characterized by Bink et al. (2003). Using morpholino anti-sense oligonucleotides to inhibit HS6ST-1 and -2 function, we show that these two proteins are required for normal patterns of 6-*O* sulfation. HS6ST-1 and HS6ST-2 display distinct expression patterns in vivo. HS6ST-2 is expressed in the region around the caudal vein, and HS6ST-2 morphant embryos show defects in the branching morphogenesis of the caudal vein, defects which were not observed in HS6ST-1 morphant embryos. The finding that HS6ST-2 is essential for the branching morphogenesis of the caudal vein in zebrafish is the first evidence for an in vivo role of a HS6ST in vascular development of a vertebrate system.

Materials and methods

Morpholino sequences and injections

The HS6ST-1 and HS6ST-2 morpholino phosphorodiamidate oligonucleotides (morpholinos), from Gene Tools, LLC, have the following sequences:

HS6ST-1 MO #1: 5′-TCCAGTGAGGAGGTTCATGTGTTAC-3′
HS6ST-1 MO #2: 5′-GTTGACTGTTTTTTAGGGTGTCTCC-3′
HS6ST-2 MO #1: 5′-GATTTCCCATCCATCTTCTCGCTGG-3′
HS6ST-2 MO #2: 5′-AGTGAAAGCATTACTCGGTTGTGCG-3′
VEGF-A MO: 5′-GTATCAAATAAACAACCAAGTTCAT-3′
VEGF-A MOd4 (four-base mismatches are in lower-case): 5′-GTAaCAAtTAAACAACCAtGTTgAT-3′

All were designed against the corresponding cDNA (see GenBank accession numbers below). All morpholinos were prepared and injected as previously described (Nasevicius and Ekker, 2000). HS6ST-2 MO #1 is identical to the HS6ST MO #1 described by Bink et al. (2003) and HS6ST-2 MO #2 is shifted one base 5′ of their second HS6ST-2 targeted morpholino. VEGF-A morpholinos are from Nasevicius et al. (2000).

Raising and staging embryos

Embryos were raised at 29°C. Zebrafish embryos were staged using standard morphological criteria (Kimmel et al., 1995) prior to fixation and analysis to compensate for any observed developmental delay.

Microangiography analysis

For microangiography analysis, tetramethylrhodamine isothiocyanate (TRITC)-dextran dye was dissolved in 0.3 × Danieau buffer (58 mM NaCl, 0.7 mM KCl, 0.4 mM $MgSO_4$, 0.6 mM $(CaNO_3)_2$, 5.0 mM HEPES pH 7.6) at 20 mg/ml and was microinjected into the common cardinal vein of Tg(fli-1:EGFP) embryos as previously described (Nasevicius et al., 2000). The fli-1:EGFP-labeled vasculature and the microangiograms were visualized using the FITC and the TRITC filter sets as previously described (Finley et al., 2001).

Cloning of zebrafish HS6ST-1 and HS6ST-2

The full-length coding sequence for zebrafish HS6ST-1 and HS6ST-2 was determined by standard sequencing of EST clones obtained from Incyte Genomics. The cDNA sequences were submitted to GenBank (HS6ST-1: AY575770; HS6ST-2: AY575769).

Expression constructs and injections

A *Spe*I site was introduced at the 5′ and the 3′ ends of the zebrafish HS6ST-1 and HS6ST-2 coding sequence by PCR, using the EST clones as the DNA template. The PCR fragment was subsequently subcloned into the *Spe*I site of the FRM expression construct (Gibbs and Schmale, 2000). DNA-based rescue of morpholino-induced defects was conducted using the methods essentially as previously described for *syndecan-2* (Chen et al., 2004). The solution of the test DNA construct mixed with FRM-DsRed expression construct was injected into 1-cell embryos at the interface between the yolk and the blastomere to ensure uniform mosaic distribution (Finley et al., 2001). The FRM-DsRed expression construct is used as a lineage tracer to facilitate the selection of embryos showing mostly uniform mosaic expression.

Preparation and HPLC analysis of heparan sulfate disaccharides

This protocol was adapted from Toyoda et al. (2000) and Ledin et al. (Unpublished, Uppsala University, Sweden). Samples of 100, 48 hpf dechorionated zebrafish were washed in distilled water and lyophilized, then resuspended in 0.5 ml 50 mM Tris/HCl pH 8, 1 mM $CaCl_2$, 1% Triton-X100. The samples were sonicated three times for 30 s at 4–5 W before removal of a fraction of material for protein estimation (Pierce BCA Assay). Samples were then digested with 0.8 mg/ml protease for 16 h at 55°C, heat inactivated at 96°C for 5 min, then incubated 2 h at 37°C with 1 μl 1 M $MgCl_2$ and 0.5 μl (168.5 U) benzonase. NaCl was added to 0.1 M and insoluble material removed by microcentrifugation for 10 min at 16,000×*g*. The solution was applied on a Vivapure Mini D membrane (Sartorius AG, Germany), which had been equilibrated with sodium phosphate buffer (pH 6.0) containing 0.15 M NaCl. The fractions eluted with 1.0 M NaCl in the same buffer were collected, desalted with Biomax-5 (Millipore, Billerica, MA) filtration column, lyophilized and resuspended in 15 μl 0.03 M sodium acetate buffer (pH 7.0) with 3.33 mM calcium acetate, 0.33 mIU heparinase, 0.33 mIU heparitinase II and 0.33 mIU heparitinase I (Seikagaku America, East Falmouth, MA). The mixture was incubated at 37°C for 16 h, lyophilized and resuspended in 12 μl water to load onto the HPLC. HPLC conditions were as Toyoda et al., 2000.

In situ hybridization

A *Bgl*II site was introduced at the 5′ and the 3′ ends of the zebrafish HS6ST-2 coding sequence by PCR, and the DNA fragment was subcloned into the *Bgl*II site of T3TS (Hyatt and Ekker, 1999). The plasmid was linearized with *Spe*I and T3 polymerase was used for DIG-labelled antisense RNA synthesis. The PCR fragment containing the open reading frame of HS6ST-1 was subcloned into the TOPO vector (Invitrogen). The plasmid was linearized with *Spe*I, and T7 polymerase was used for DIG-labelled antisense RNA synthesis. DIG-labelled probes were synthesized using the in vitro DIG labelling kit (Roche). The in situ hybridization procedure was performed essentially as described (Jowett, 1999).

Results

In our ongoing morpholino-based screen to identify novel genes essential for vascular development in the zebrafish, *Danio rerio*, we characterized vascular defects in embryos injected with morpholinos against a gene fragment with similarity to vertebrate HS6ST proteins. Upon full sequencing of the target cDNA (Fig. 1A) and subsequent phylogenetic analysis (Fig. 1C), the gene target was later identified as a zebrafish HS6ST-2 family member. From the zebrafish EST database, one other HS6ST-related gene was identified. Sequence (Fig. 1B) and phylogenetic analysis (Fig. 1C) of the full-length coding sequence for this

A

```
MDGKSNYSRL LIALLMILFF GGIVLQYICS TSDWQLLHLA  40
SLSSRLGSRA PGDRLNGAGA GDPYSSEDGA LVRFVPRFNF  80
TTKDLSRAVD FHIKGDDVIV FLHIQKTGGT TFGRHLVRNI 120
QLERPCECHA GQKKCTCYRP GKRDTWLFSR FSTGWSCGLH 160
ADWTELTNCV PSFMSNRESQ ERRMTPSRNY YYITILRDPV 200
WRYLSEWRHV QRGATWKASK HMCDGRLPTL TELPSCYPGD 240
DWSGCSLEEF MVCPYNLANN RQTRMLADLS LVGCYNLTVM 280
SENQRWAMLL ESAKRNLRNM AFFGLTEYQR KTQYLFEHTF 320
RLSFIAPFTQ LNGTRAASVE VEPETQRRIR ELNQWDVELY 360
EYARDLFLQR FQFARQQERR EARQRRIQER RKLRAKVKSW 400
LGVTGKAVFK PTKEPPMTEQ SPAFAEEKQA DAEQTLESET 440
EGQVEENWLE EDDGEIMLDY SENVEQWR              468
```

B

```
MVERSSKFLF IVVGSVLFML ILYQYVAPGM MNFGSPHGYM  40
LEDDADLFPT PDPHYVKKFY FPIRDLERTV DFEIKGDDVI  80
VFLHIQKTGG TTFGRHLVQN VRLEVPCDCR PGQKKCTCYR 120
PNRKETWLFS RFSTGWSCGL HADWTELTNC VPGVLNKKES 160
RMKNQRKFYY ITLLRDPVSR YLSEWRHVQR GATWKTSLHM 200
CDGRTPTPEE LPPCYEGTDW SGCTLQQFMD CPYNLANNRQ 240
VRMLADLSLV GCYNMSFIPE KKRAQVLLES AKKNLRDMAF 280
FGLTEFQRKT QYLFERTFRL KFIRPFMQYN STRAAGVDLD 320
NDTIQRIEEL NDLDMQLYDY ARDLFQQRYM YKRQLERREQ 360
RLKNQPLFPF RRTSSSDSTF RDDAPESEGS RLPTEDYMNH 400
IINRW                                       405
```

C

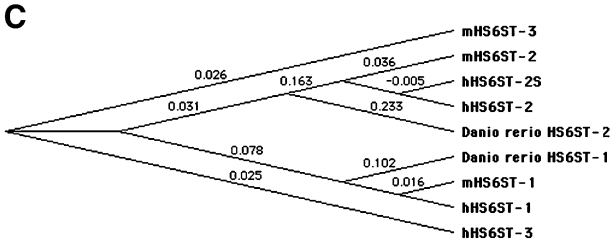

Fig. 1. Identification of zebrafish HS6ST-1 and HS6ST-2 genes. (A) Deduced amino acid sequence of zebrafish HS6ST-2 (A) and zebrafish HS6ST-1 (B) genes. The putative PAPS binding sites are underlined. (C) Phylogenetic tree of vertebrate HS6ST proteins assembled using CLUSTAL analysis (Macvector 7.2.3 software). The value at each branch denotes the mean number of differences per residue along each branch (Thompson et al., 1994). Human HS6ST-2 S is an alternate isoform of HS6ST-2 (Habuchi et al., 2003).

additional HS6ST gene indicates that this is a zebrafish HS6ST-1 family member. We have conducted subsequent analyses of the EST and genomic databases, and we have identified fragments of sequence that code for possibly two additional members of the zebrafish HS6ST gene family; sequence coverage is, however, not sufficient to unambiguously assign likely orthology (data not shown).

The embryonic expression pattern of HS6ST-1 is distinct from that of HS6ST-2 in zebrafish

To determine whether zebrafish HS6ST-1 and HS6ST-2 might have distinct biological roles, in situ hybridization was conducted to compare spatial expression patterns during development. A previous report by Bink et al. (2003) demonstrated expression of HS6ST-2 in the brain during somitogenesis and at 24 h post-fertilization (hpf) and also in the fin buds at 48 hpf (Bink et al., 2003). Here, we show that expression of HS6ST-2 is also detected in the caudal wave of maturing somites from the 4-somite stage to the 18 somite-stage (arrowheads in Figs. 2A–C and data not shown). At the 22-somite stage, HS6ST-2 is detected in a stripe of cells in ventral medial somites (Fig. 2D) and persists through 24 hpf (Fig. 2E). A transverse section through the caudal region of an embryo at 24 hpf indicates expression of HS6ST-2 in the ventral medial somites and cells surrounding the vascular structures of the dorsal aorta and caudal vein in the tail (area of expression outlined by dash lines in Fig. 2F).

Similar to HS6ST-2 (Fig. 2E), HS6ST-1 is also strongly expressed in the eyes during somitogenesis (Figs. 2G–H). In contrast to HS6ST-2, localized expression of HS6ST-1 mRNA in the brain is detected during somitogenesis, at 24 hpf and 33 hpf (Figs. 2I–K), and its expression is not detected in the vasculature.

Analysis of heparan sulfate composition of HS6ST morphants

To determine if HS6ST-1 and HS6ST-2 function affects the structural modifications of heparan sulfate in vivo, glycosaminoglycans were isolated from wild-type, buffer-injected and morpholino-injected embryos. The partially purified heparan sulfate was digested with heparin lyases into disaccharides. The disaccharides were then separated by reverse phase ion pair HPLC and labeled with post-column fluorescent derivatization. The peaks were identified by their elution time compared to that of known heparan sulfate disaccharide standards. Six disaccharide species, including three 6-*O* sulfated disaccharides, ΔUA-GlcNAc6S, ΔUA-GlcNS6S and ΔUA2S-GlcNS6S, (see Fig. 3 legend for key to abbreviations) were present in wild-type, buffer-injected, and morpholino-injected embryos (Fig. 3, data not shown). Two of the three 6-*O* sulfated disaccharides, ΔUA-GlcNAc6S and ΔUA-GlcNS6S (peaks 3 and 4, Fig. 3B), were significantly reduced in both HS6ST-1 MO- and HS6ST-2 MO-injected embryos compared to wild-type embryos (see Table 1). The relatively modest changes observed with morpholino knockdown of either HS6ST-1 or HS6ST-2 are possibly due to functional redundancy between HS6ST genes in zebrafish, of which only one was targeted at a time. When both HS6ST-1 and HS6ST-2 genes were simultaneously targeted using a reduced dosage inhibition protocol to allow embryo viability, there was no additional decrease in the 6-*O*-sulfated disaccharides (data not shown). This result suggests that there are other HS6ST genes in the zebrafish that may be able to compensate for the remaining 6-*O* sulfotransferase function. The limited effects of the morpholinos may also be attributed to the low doses that were used to avoid any non-specific toxicity. There was no change in HS-derived disaccharides from buffer-injected embryos compared to wild-type controls indicating the changes observed in heparan sulfate composition were not a result of stress to the embryo due to the injection (Table 1). These results suggest that both HS6ST-1 and HS6ST-2 can sulfate similar disaccharide species, although these disaccharides may be present within a different oligosaccharide sequence, since the disaccharide profiling does not provide information concerning the structural context of any given disaccharide.

HS6ST-2 MO-injected embryos showed defective morphogenesis of the caudal vein

In our morpholino-based screen, an EGFP transgenic line (fli-1:EGFP) was used to assess vascular development. In Tg(fli-1:EGFP) embryos, the fli-1 promoter drives the expression of the EGFP reporter in endothelial cells that line the blood vessels (Lawson and Weinstein, 2002). At 24 hpf, no apparent vascular defects were observed in HS6ST-2 MO-injected embryos. Beginning around 30 hpf, however, HS6ST-2 MO-injected Tg(fli-1:EGFP) embryos showed defective formation of the venous plexus, the network of microvessels derived from the caudal vein (CV) (Fig. 4). In the less severe case, HS6ST-2 MO-injected embryos displayed reduced branching of the CV. Instead of the fine meshwork of the CV observed in uninjected wild-type embryos, HS6ST-2 MO-injected embryos exhibited the formation of large loops in the CV plexus (arrowheads in Fig. 4C). In the more severe case, HS6ST-2 MO-injected embryos showed a lack of branching and instead formed disorganized and over-lumenized vessels in place of the venous plexus (arrowheads in Fig. 4E). In contrast, no vascular defects were observed in embryos injected with the HS6ST-1 morpholino at a dose where a change in the 6-*O* sulfation profile was observed (Fig. 3 and Table 1), consistent with the lack of HS6ST-1 expression in the developing vasculature. The expression of HS6ST-1 in the developing eyes and the central nervous system suggest that HS6ST-1 may play a role in other biological functions during development.

To assess the functional integrity of the vasculature (for example, leakiness of vessel walls and lumen patency), microangiography was conducted on HS6ST-2 MO-injected embryos using TRITC-dextran. Functional circulation was observed in HS6ST-2 MO-injected embryos showing reduced branching morphogenesis of the CV (Fig. 4D). In the most severe case, pooling of TRITC-dextran was observed in the cavernous vessels that lack any branching morphology (Fig. 4F).

To assess whether the defective morphogenesis of the CV was specific to the loss of HS6ST-2 function, we showed that two gene-specific morpholinos of independent

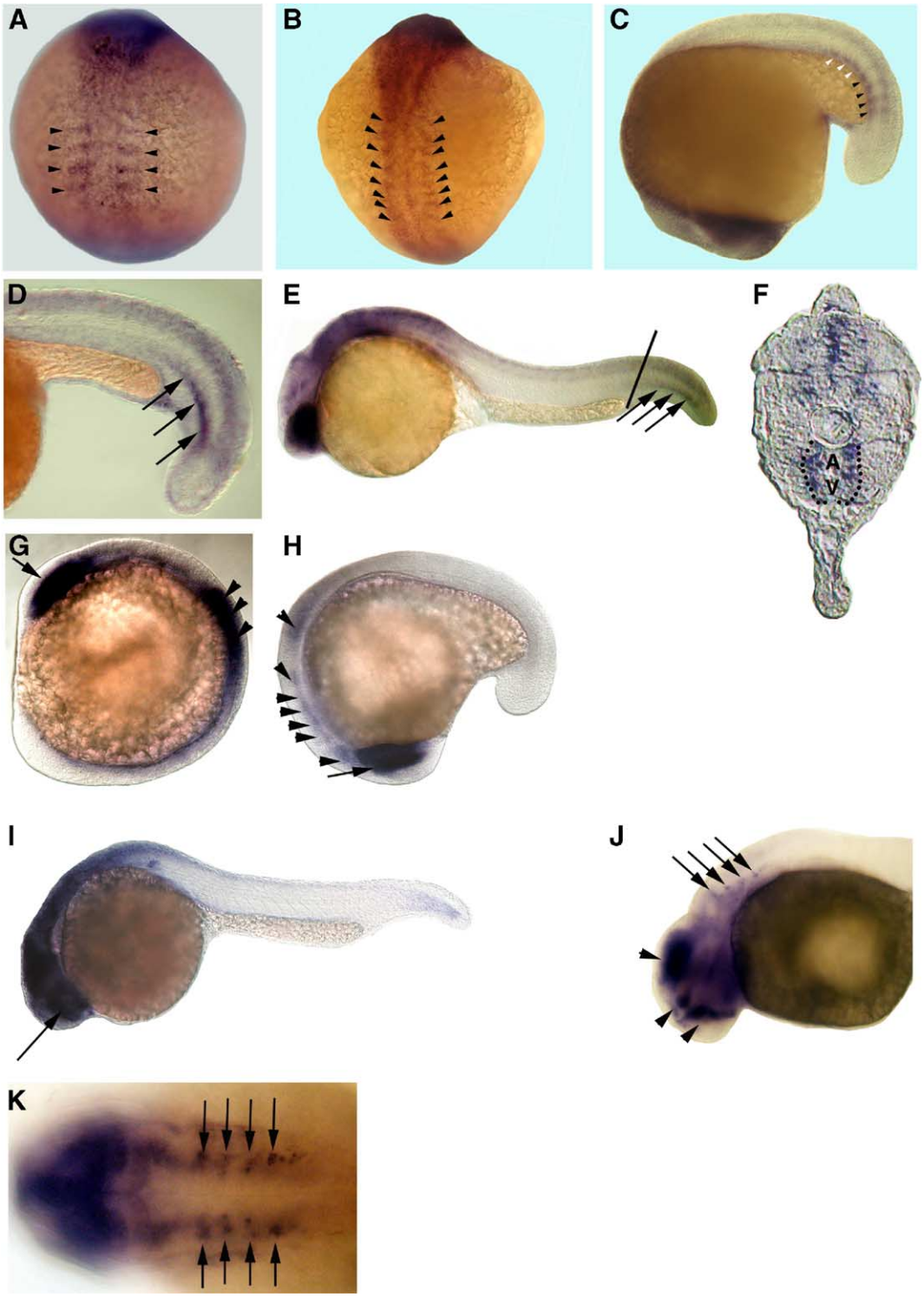

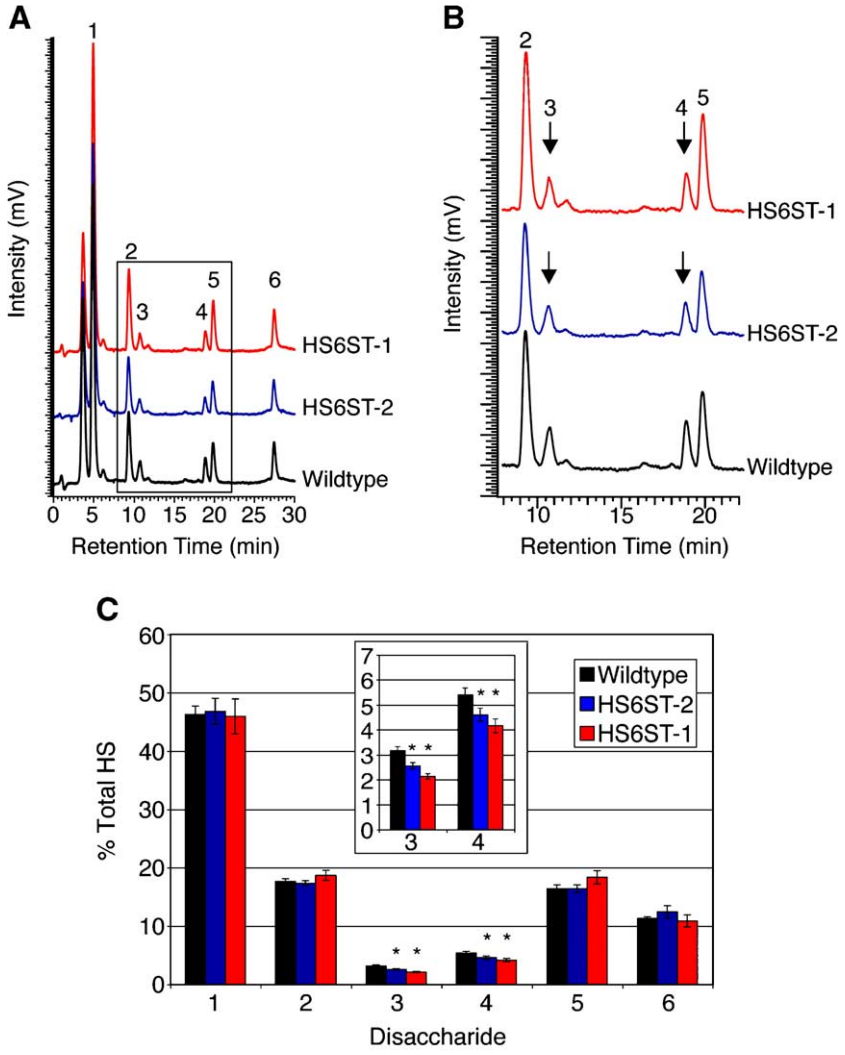

Fig. 3. Heparan sulfate disaccharide profiling of HS6ST-1 and HS6ST-2 morphant embryos. (A) Representative HPLC chromatograms of wild-type (black), 5 ng HS6ST-2 morpholino-injected (blue) and 2 ng HS6ST-1 morpholino-injected (red) embryos. Six disaccharides were identified: peak 1: ΔUA-GlcNAc, Δ4,5 unsaturated hexuronate-*N*-acetyl glucosamine; peak 2: ΔUA-GlcNS, ΔUA-*N*-sulfated glucosamine; peak 3: ΔUA-GlcNAc6S, ΔUA-6-*O*-sulfated GlcNAc; peak 4: ΔUA-GlcNS6S, ΔUA-6-*O*-sulfated GlcNS; peak 5: ΔUA2S-GlcNS, ΔUA2-*O*-sulfated GlcNS; peak 6: ΔUA2S-GlcNS6S. (B) Boxed region of (A). Arrows represent the two 6-*O* sulfated disaccharides, peak 3 and peak 4, which are reduced in HS6ST-1 and HS6ST-2 morpholino-injected embryos. (C) Graphical depiction of disaccharide composition in wild-type (black), HS6ST-2 (blue) and HS6ST-1 (red) morpholino-injected embryos, represented as percent of total heparan sulfate. Inset is close up of peaks 3 and 4, ΔUA-GlcNAc6S and ΔUA-GlcNS6S, respectively. Asterisks indicate significant changes from wild-type (*t* test $P < 0.05$ with HS6ST-1 peak 3 $P < 0.001$).

sequence generated similar defects in the plexus of the CV including the formation of large loops in the plexus and enlarged vascular channels (Fig. 4G). In contrast, injection of HS6ST-1 MO at a similar dose range did not generate a significant percentage of embryos with caudal vein defects (compare column 3 to columns 1 and 2 in Fig. 4G). We

Fig. 2. Embryonic expression patterns of zebrafish HS6ST-1 and HS6ST-2 mRNA. (A) 4-somite stage. (B) 10-somite stage. (C) 16-somite stage. Zebrafish HS6ST-2 is expressed in the forming somites (arrowheads in panels A–C). HS6ST-2 expression is down-regulated in more differentiated somites (white arrowheads in C). (D) At 22-somite stage (20 hpf), zebrafish HS6ST-2 is expressed in a stripe of cells in somitic mesoderm (arrows). (E) At 24 hpf, expression of zebrafish HS6ST-2 is detected in the eyes, the brain and ventral medial somites in the tail. (F) A transverse section of the embryo in (E). Zebrafish HS6ST-2 expression is detected in the ventral medial somites and cells surrounding the dorsal aorta (A) and posterior cardinal vein (V) in the tail (as outlined by the dashlines). The level of the section is indicated by the line in (E). (G) At 10-somite stage, zebrafish HS6ST-1 is expressed in the optic vesicles (arrow) and the neural tube (arrowheads). (H) At 16-somite stage, zebrafish HS6ST-1 is expressed in the developing eyes (arrow), the tegmentum, the forming rhombomeres and the neural tube (arrowheads). (I) At 24 hpf, expression of zebrafish HS6ST-1 is detected in the eyes (arrow), the brain and the neural tube. (J) At 33 hpf, expression of zebrafish HS6ST-1 is detected in the diencephalon, the telencephalon, the tegmentum (arrowheads) and in four bilateral patches of cells at the level of the dorsal rhombomeres (arrows). (K) Dorsal view of the embryo in (J), showing the four bilateral stripes of cells in the rhombomeres (arrows). (A–B) Dorsal view, anterior to the top. (C, H) Lateral view, anterior to the bottom. (D–E, I–J) Lateral view, anterior to the left. (G) Lateral view, anterior to the top left. (K) Anterior to the left.

Table 1
Quantification of heparan sulfate disaccharide profiles

Disaccharide	pg HS/μg protein				% Change from wild-type	
	Wild-type	Buffer	HS6ST-2 MO	HS6ST-1 MO	HS6ST-2 MO	HS6ST-1 MO
ΔUA-GlcNAc	6.4 ± 0.5	7.2 ± 0.3	5.7 ± 0.3	6.1 ± 0.5	−12 ± 7	−8 ± 2
ΔUA-GlcNS	2.4 ± 0.1	2.3 ± 0.3	2.1 ± 0.1	2.5 ± 0.1	−13 ± 5	+1 ± 10
ΔUA-GlcNAc6S	0.44 ± 0.04	0.53 ± 0.01	0.32 ± 0.03	0.28 ± 0.01	−28 ± 4*	−36 ± 4*
ΔUA-GlcNS6S	0.75 ± 0.06	0.78 ± 0.05	0.57 ± 0.05	0.55 ± 0.03	−24 ± 8*	−27 ± 9*
ΔUA2S-GlcNS	2.25 ± 0.09	2.4 ± 0.5	2.0 ± 0.1	2.4 ± 0.2	−10 ± 5	+8 ± 8
ΔUA2S-GlcNS6S	1.6 ± 0.1	1.71 ± 0.09	1.5 ± 0.2	1.4 ± 0.1	−3 ± 16	−8 ± 17
Total	14 ± 1	14.9 ± 0.2	12.27 ± 0.07	13.18 ± 0.04	−12 ± 7	−6 ± 7

Average pg HS/μg protein from two individual experiments wild-type $n = 7$ samples, injected $n = 4$ samples. Each sample contains ~100 embryos. ±SEM.
* Values significantly different from wild-type ($P \leq 0.05$ t test).

also asked whether the introduction of the HS6ST-2 protein would alleviate the vascular defects observed in HS6ST-2 MO-injected embryos. A mixed solution of HS6ST-2 DNA expression construct that does not contain the HS6ST-2 MO binding site and a DsRed construct was co-injected with HS6ST-2 MO into Tg(fli-1:EGFP) embryos. DsRed is introduced as a tracer to facilitate the identification of DNA-injected embryos (Fig. 5D). In this method, DNA injection results in the mosaic distribution of inherited DNA in these embryos (Fig. 5D). Compared to embryos injected with the HS6ST-2 MO alone, a higher frequency of the co-injected embryos showed normal formation of the caudal vein plexus (Fig. 5F, compare the second column to the first columns, $P < 0.0005$). In co-injected embryos, HS6ST-2-expressing cells correlated with regions in the restored venous plexus (Fig. 5E). In contrast, co-injection of a control expression construct did not affect the frequency of vascular defects in HS6ST-2 MO-injected embryos (Fig. 5F, compare column 3 to column 1, $P > 0.2$). These results indicate that the venous defects observed in embryos injected with HS6ST-2 MO are specific to the loss of HS6ST-2 function.

HS6ST-2 is required for somite development

A previous report by Bink et al. (2003) has demonstrated that zebrafish HS6ST-2 plays a role during the late stage of anterior somite patterning as indicated by the reduced expression of *mesp-b*, a bHLH transcription factor upstream of notch5 and notch6 in zebrafish, in HS6ST-2 morphant embryos. HS6ST-2 is also essential for proper muscle differentiation. In wild-type embryos, high expression of *myoD* is only detected in posterior-most somites at 24 hpf. In contrast, *myoD* expression remains upregulated in all somites of HS6ST-2 morphant embryos at 24 hpf (Bink et al., 2003). We have also observed similar alterations in the expression of *mesp-b* (34% ± 7%, $n = 49$, ±SEM) and *myoD* (67% ± 17%, $n = 46$, ±SEM), supporting the role of HS6ST-2 in muscle development. These noted defects in somitogenesis correlate with the somitic wave of HS6ST-2 expression during segmentation (Figs. 2A–E).

Expression of late endothelial markers is reduced in HS6ST-2 morphants

To assess the nature of the vascular defects in HS6ST-2 morphants, in situ hybridization was conducted to analyze expression of endothelial markers in HS6ST-2 morphants during vascular development. Expression of *flk-1*, which encodes a Vascular Endothelial Growth Factor (VEGF) receptor, is first detected in bilateral stripes of endothelial precursor cells during early somitogenesis and becomes localized to the endothelium of developing blood vessels from late somitogenesis to about 36 hpf (Fouquet et al., 1997). Compared to uninjected wild-type embryos, *flk-1* expression was normal in HS6ST-2 morphants at 24 hpf (Fig. 6B), indicating that the primary formation of the axial vessels and initial sprouting of intersegmental vessels proceed normally in HS6ST-2 morphants.

In a zebrafish embryo, branches from the developing caudal vein are observed at 30 hpf and form a plexus up to 40 hpf. The caudal vein is subsequently remodeled to form a single vascular tube by day 5 post-fertilization (Isogai et al., 2001; Huang et al., 2003). The vascular markers, *tie-1* and *tie-2*, are expressed in the endothelium of the vasculature undergoing this angiogenic remodeling process (Lyons et al., 1998). Expression domains of *tie-1* and *tie-2* were reduced in the developing caudal vein of HS6ST-2 MO-injected embryos at 30 hpf (arrowheads in Fig. 6D and data not shown; compare to uninjected control, Fig. 6C) and at 48 hpf (data not shown). These results indicate that the venous defects observed in HS6ST-2 morphants occur during latter stages of vascular development in zebrafish embryos.

HS6ST-2 and VEGF interact in vivo during caudal vein plexus formation

VEGF-A is one of several heparin-binding growth factors that play an essential role in angiogenesis. To assess for an in vivo interaction between HS6ST-2 and VEGF-A during caudal vein plexus formation, morpholinos against HS6ST-2 and VEGF-A were co-injected into embryos using doses that alone elicited only minimal effects on venous

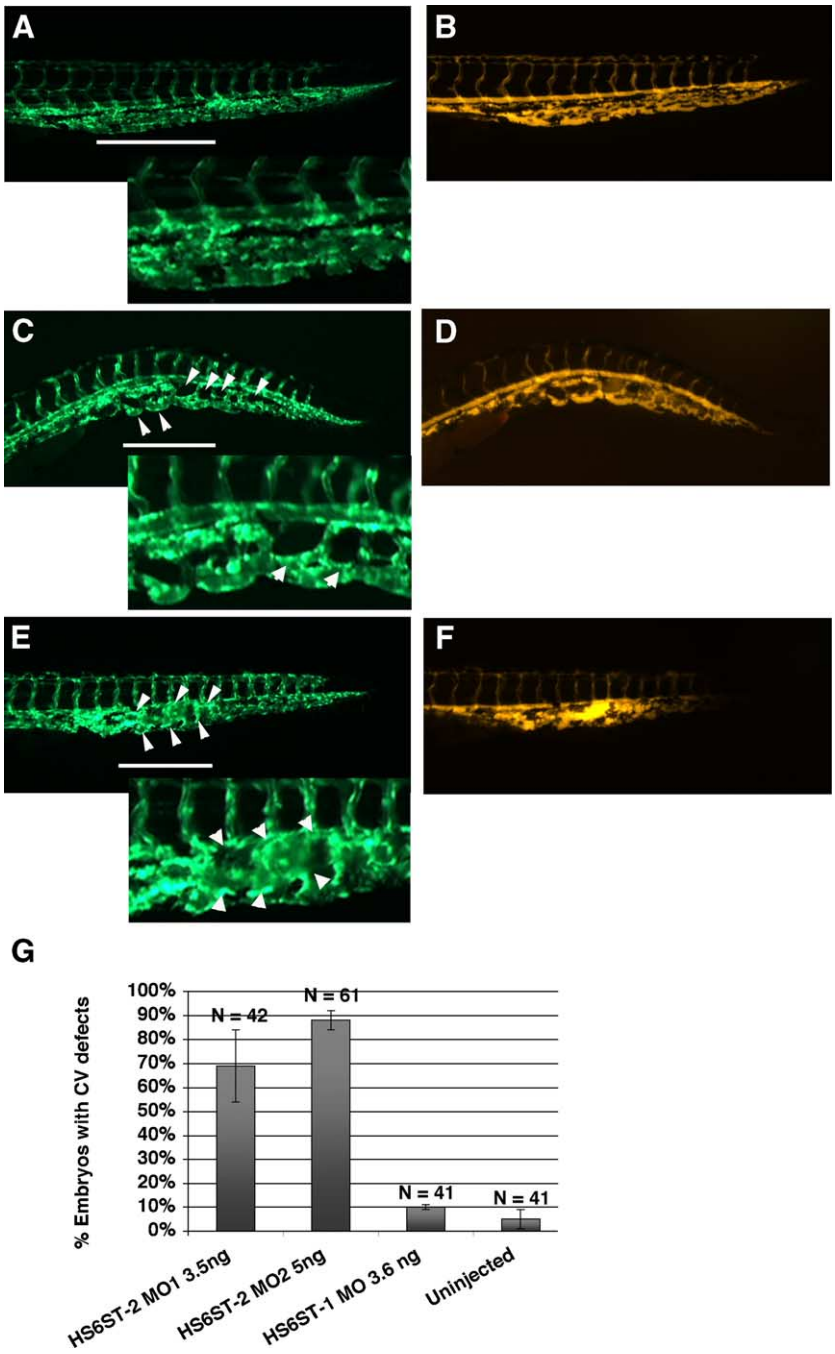

Fig. 4. Zebrafish HS6ST-2 is essential for branching morphogenesis of the caudal vein in zebrafish embryos. (A) Tg(fli-1:EGFP) embryo at 48 hpf under FITC illumination with inset at the lower left corner showing a region of the venous plexus. (B) Angiogram of the Tg(fli-1:EGFP) embryo in (A) under TRITC illumination. (C–D) Tg(fli-1:EGFP) embryo injected with 5 ng of HS6ST-2 MO2 (C) and the angiogram of the same embryo (D) showing reduced branching as indicated by large loops (arrowheads) in the caudal vein plexus. (E–F) In the more severe case, the venous plexus in a Tg(fli-1:EGFP) embryo fails to achieve the complexity as observed in Tg(fli-1:EGFP) embryos. Instead, the formation of a cavernous vessel (arrowheads) is observed. (G) A summary graph showing results of injections using two non-overlapping morpholinos against the zebrafish HS6ST-2 gene. Both oligos generate similar cardinal vein defects including formation of large loops and cavernous vessels with high penetrance. In contrast, HS6ST-1 MO (column 3) does not generate a significant percentage of embryos with CV defects. CV, cardinal vein. *N* denotes the number of embryos analyzed. ±SEM. The lines in panels A, C and E indicate the segments of venous plexus displayed in insets.

plexus formation (Figs. 7B, C and F). Compared to single injection of either HS6ST-2 MO or VEGF-A MO alone, co-injection of HS6ST-2 MO and VEGF-A MO resulted in synergistic increase in the frequency of embryos with caudal vein branching defects, i.e., formation of large loops and cavernous vessels (Fig. 7F, column 3; see examples in Figs. 7D–E). Co-injection of HS6ST-2 MO and a four-base mismatch VEGF-A MO (d4) abolished the synergy (Fig. 7F,

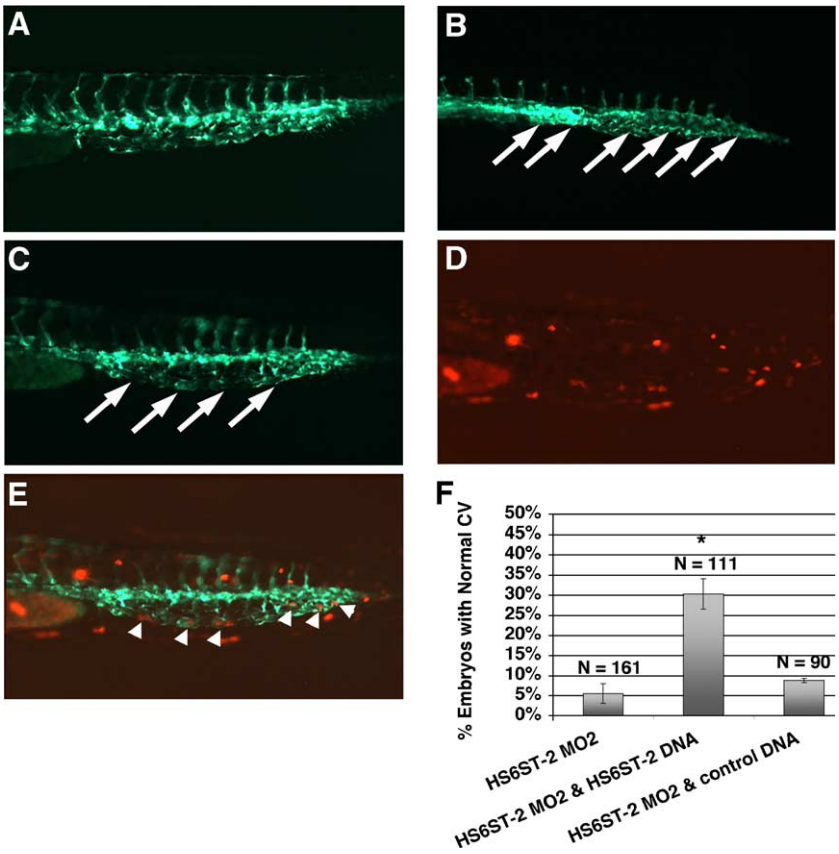

Fig. 5. Co-injection of zebrafish HS6ST-2 expression construct alleviates the caudal vein defects in HS6ST-2 morphant embryos. (A) Uninjected Tg(fli-1:EGFP) embryo at 33 hpf under FITC illumination. (B) HS6ST-2 MO2-injected embryo with defective caudal vein branching as indicated by the formation of a cavernous vessel (arrows). (C) Embryo co-injected with HS6ST-2 MO2 and a mixed solution of HS6ST-2 DNA and DsRed DNA, showing the restoration of the venous plexus (arrows) under FITC illumination. DsRed is introduced as a tracer to facilitate the identification of DNA-injected embryos. (D) DsRed expression in the same co-injected embryo showing mosaic expression pattern in the tail under TRITC illumination. (E) Overlay of panels C and D, showing DsRed expressing-cells, correlating with areas in the restored venous plexus (arrowheads). (F) Summary of four independent co-injection experiments. The test DNA (HS6ST-2 expression construct) or the control DNA (DsRed expression construct) was injected into embryos separately injected with HS6ST-2 MO2. The introduction of HS6ST-2 protein by the DNA injection alleviates the caudal vein defects in HS6ST-2 MO2-injected embryos (compare column 2 to column 1). Asterisk (*) denotes statistical significance with $P < 0.0005$. In contrast, a separate injection of control DNA into HS6ST-2 MO2-injected embryos does not affect the frequency of caudal vein defects in HS6ST-2 MO2-injected embryos (compare column 3 to column 1; $P > 0.2$). *N* indicates the total number of embryos scored. ±SEM.

column 4). These results suggest that HS6ST-2 and VEGF-A interact in vivo during caudal vein formation.

Discussion

The specific sulfation pattern of heparan sulfate is essential for its ability to interact with a variety of heparin-binding growth factors involved in angiogenesis. While 6-*O* sulfation has been implicated in vessel formation in vitro (Lundin et al., 2000), the in vivo function of 6-*O* sulfation in vascular development is poorly understood. In this study, we have used zebrafish as a vertebrate model system to understand the role of 6-*O* sulfation in vascular development. We have examined the function of two HS6ST genes, HS6ST-1 and HS6ST-2. Structural analyses of heparan sulfate disaccharides isolated from HS6ST-1 and HS6ST-2 morphants indicated that these two enzymes are required for the normal 6-*O* sulfation pattern of heparan sulfate. HS6ST-1 and HS6ST-2 display distinct expression patterns. HS6ST-2 is expressed in the region of the developing caudal vein and is required for the branching morphogenesis of the caudal vein. This study provides the first in vivo evidence of a heparan sulfate modifying gene, HS6ST-2, being essential for vascular development.

Distinct expression patterns and functions for HS6ST-1 and HS6ST-2

In situ hybridization revealed dynamic, highly localized expression patterns of HS6ST-1 and HS6ST-2 during development. The expression of HS6ST-2 in the cells surrounding the dorsal aorta and posterior cardinal vein suggested that it might have a role in vascular development or function. This was substantiated by the reduced

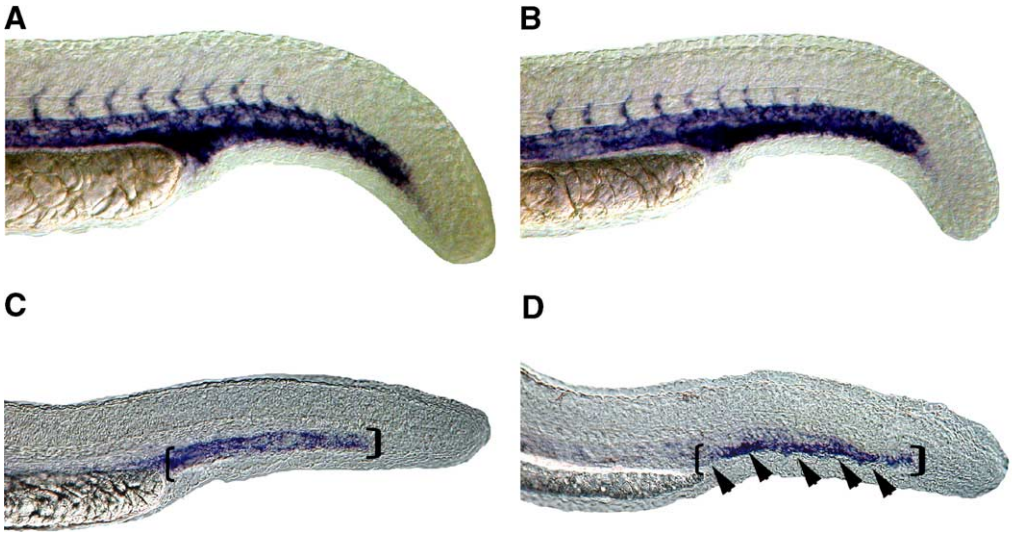

Fig. 6. Expression of late endothelial markers in the region of forming venous plexus is reduced in HS6ST-2 morphants. Expression of *flk-1* as shown by whole-mount in situ hybridization in a wild-type embryo (A) and a HS6ST-2 MO-injected embryo (B) at 24 hpf. Normal expression of *flk-1* is observed in HS6ST-2 MO-injected embryos at 24 hpf (n = 19). However, at 30 hpf, the expression domain of the late endothelial marker, *tie-1* (D; 81% ± 8%, n = 40, ±SEM) is reduced in the region of caudal vein (area indicated by brackets and arrowheads) in HS6ST-2 MO-injected embryos compared to wild-type embryos (C).

branching complexity in the caudal vein plexus observed in HS6ST-2 morphants. Our analysis of HS6ST-2 expression in the developing somites also supports a role in muscle development, as previously proposed (Bink et al., 2003). In contrast, morpholino knockdown of HS6ST-1 did not affect vascular development, and its expression pattern indicates that it may be important for eye and brain development.

Compositional analysis of heparan sulfate from HS6ST morpholino antisense knockdown embryos

Biochemical analysis of heparan sulfate from morphant embryos demonstrated that both HS6ST-1 and HS6ST-2 affect 6-*O*-sulfation of both *N*-sulfoglucosamine and *N*-acetyl glucosamine. In contrast, cell free assays of HS6STs (Habuchi et al., 2000, 2003; Bink et al., 2003) suggested that these enzymes exhibit poor activity towards *N*-acetyl glucosamine (Habuchi et al., 2000). Similarly Bink et al. (2003) observed very little sulfation of *N*-acetyl glucosamine by zebrafish HS6ST-2 extracted from COS-7 cells. In vivo analysis, however, from our study and that of Bink et al. (2003) suggest that HS6STs can affect 6-*O* sulfation of *N*-acetyl glucosamine. Compared to Bink et al. (2003), we noted less of a decrease in the disaccharide ΔUA-GlcNS6S and no significant decrease in ΔUA2S-GlcNS6S upon morpholino knockdown of HS6ST-2, perhaps due to our use of only one of the two morpholino sequences they used or to possible strain/staging specific differences in the wild-type disaccharide profiles. Interestingly, in both studies, the level of ΔUA2S-GlcNS6S, found to be critical for heparan sulfate binding of a number of proteins (Feyzi et al., 1997; Parthasarathy et al., 1994), was preserved to a greater extent than the other 6-*O*-sulfated disaccharides in the morphant embryos. This may represent a mechanism to retain specific ligand binding properties of heparan sulfate at low enzyme levels. It is likely that the recognition site for the HS6STs in vivo is more complex than the individual substrate disaccharide type, and its activity depends on the surrounding sequence having the correct structural features (Zhang et al., 2001, Smeds et al., 2003, Jemth et al., 2003). Although we were not able to detect disaccharide type specificity for zebrafish HS6ST-1 and HS6ST-2, their substrate recognition sites may be unique to the heparan sulfate of the separate tissues in which they are expressed. Our results suggest that the tissue-specific expression of the HS6STs may contribute to their unique biological functions.

Analysis of the role of HS6ST-2 in angiogenesis

In this study, the role of HS6ST-2 in angiogenesis is explored. As the primary vasculature is laid down in a vertebrate embryo, the primitive network of blood vessels undergoes a series of remodeling steps to form mature vasculature, which is further stabilized by the recruitment of smooth muscle cells and other supporting cells (Carmeliet, 2000). Reduced expression domains of the late endothelial markers *tie-1* and *tie-2* in the caudal vein during the time period of remodeling indicate that HS6ST-2 is important for development of the vasculature in this region. This result correlates with the reduced branching complexity of the caudal vein plexus observed in the HS6ST-2 morphant Tg(fli-1:EGFP) embryos and the location of HS6ST-2

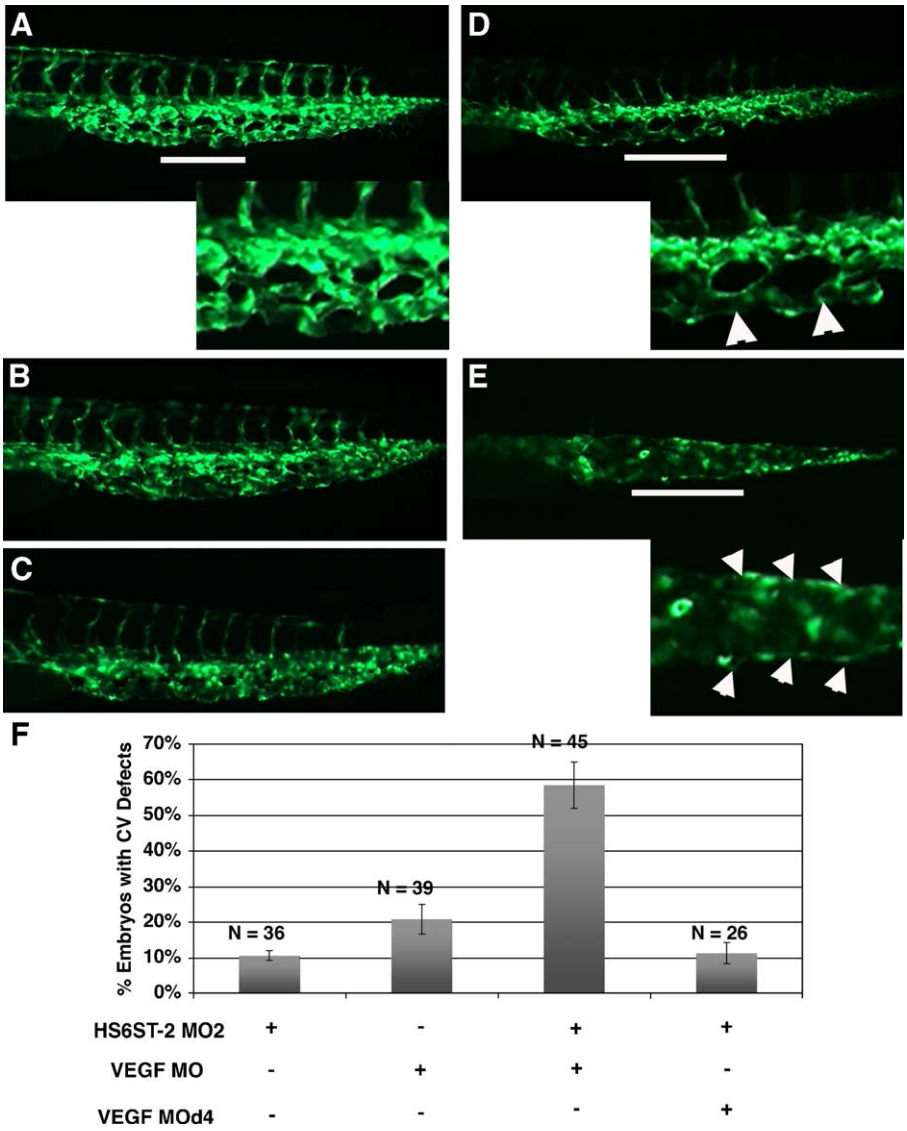

Fig. 7. HS6ST-2 and VEGF-A interact during caudal vein plexus formation in vivo. (A) Uninjected Tg(fli-1:EGFP) embryo at 33 hpf under FITC channel, with the inset displaying an enlargement of a segment in the venous plexus. (B) Embryo injected with 0.5 ng of HS6ST-2 MO2 displaying a venous plexus without any obvious defect. (C) Embryo injected with 1 ng of VEGF-A MO, displaying a venous plexus without any obvious defect. (D–E) Embryo co-injected with HS6ST-2 MO2 and VEGF-A MO displaying defective branching morphogenesis of the venous plexus as indicated by the formation of large loops (arrowheads in inset of D) and a single cavernous vessel with no branching (arrowheads in inset of E). The lines in A, D and E indicate regions in the venous plexus that are displayed in the insets. (F) A summary of two independent experiments is shown. Embryos co-injected with HS6ST-2 MO2 (0.5 ng) and VEGF-A MO (1 ng) exhibit a more than additive increase in the frequency (±SEM) of embryos with branching defects in the caudal vein plexus (column 3) compared to embryos injected with HS6ST-2 MO2 or VEGF-A MO only. In contrast, no synergy is observed in the embryos co-injected with HS6ST-2 MO and a four-base mismatch MO (d4, 1 ng) against VEGF-A (column 4).

expression at similar time points of angiogenic remodeling. The caudal vein plexus is a paradigm for studying the complexity of vertebrate angiogenesis because first it expands and then is gradually remodeled to form a single vascular tube (Isogai et al., 2001). The caudal vein phenotype we observed in the HS6ST-2 morphants is similar to that of *reg6* zebrafish mutants, which also display defects in the branching morphogenesis of the caudal vein (Huang et al., 2003). This suggests that HS6ST-2 plays an essential role in the remodeling process of the caudal vein plexus. However, we cannot exclude the possibility that defective muscle differentiation in HS6ST-2 morphant embryos may contribute to the defects of the venous plexus observed.

Role of HS6STs in branching morphogenesis

A number of studies have also provided evidence that 6-*O*-sulfated heparan sulfate may be important for the precise localization and activity of secreted modulators of branching morphogenesis. HS6STs are necessary for FGF-dependent branching morphogenesis in the *Drosophila* tracheal system and the mammalian lung (Kamimura et al., 2001; Izvolsky et al., 2003). In both cases, 6-*O*-sulfation is

predominantly in the FGF target cells, supporting its proposed requirement for FGFR activation (Pye et al., 1998; Ostrovsky et al., 2002). Spatial and temporal variance of heparan sulfate structure has been shown to facilitate assembly of specific FGF–FGFR pairs (Allen and Rapraeger, 2003). Normal vascular branch formation requires the heparin-binding sites of VEGF-A, (Ruhrberg et al., 2002), another ligand of 6-*O*-sulfated heparan sulfate (Ono et al., 1999). The ability to bind heparan sulfate has been shown to be necessary to spatially restrict VEGF to regulate vascular branching pattern (Ruhrberg et al., 2002).

We have observed a synergy between the HS6ST-2 MO and the VEGF-A MO in generating embryos with defective branching in the caudal vein, suggesting that HS6ST-2 and VEGF-A interact during angiogenesis in vivo. As *HS6ST-2* is expressed in the cells surrounding the caudal vein plexus, it is possible that the changes in the heparan sulfate modifications on the cell surface or in the extracellular matrix, induced by HS6ST-2, influence VEGF signaling by modulating the bioavailability of VEGF in the regions of the venous plexus. Another possibility is that the changes in the heparan sulfate profile induced by HS6ST-2 affect the signaling activity of other heparin-binding growth factors and in turn influence VEGF-mediated signaling. It remains to be investigated whether HS6ST-2 expression in the caudal vein plexus is important for regulating the activity of FGF or one of the many other ligands of heparan sulfate (Esko and Selleck, 2002).

In conclusion, we have demonstrated that HS6ST-1 and HS6ST-2 display distinct expression profiles and that HS6ST-2 has a unique role in vascular development. Previous in vivo studies have shown diverse roles for specific sulfate modifications of heparan sulfate in a variety of biological processes including axon guidance (Bulow and Hobert, 2004) and kidney development (Bullock et al., 1998). The results described here support the hypothesis that regulation of the sulfation pattern of heparan sulfate is a fine control mechanism of many physiological processes. Our finding that HS6ST-2 is essential for the branching morphogenesis of the caudal vein is the first in vivo evidence for a role of a specific heparan sulfate modifying enzyme in vertebrate angiogenesis. This result advocates the therapeutic benefit of agents controlling heparan sulfate modification to ameliorate a number of disorders that involve pathological angiogenesis, including tumor growth, diabetic retinopathy and coronary heart disease.

Acknowledgments

This work was supported by NIH grants to S.C.E. (GM55877 and GM63904), and an NCI grant (CA91290) and Harrison Chair Endowment to S.B.S. M.A.R and E.C. are sponsored by the MCDB and G graduate program, and E.C. was also sponsored by the combined MD/PhD training program.

References

Allen, B.L., Rapraeger, A.C., 2003. Spatial and temporal expression of heparan sulfate in mouse development regulates FGF and FGF receptor assembly. J. Cell Biol. 163, 637–648.

Bernfield, M., Gotte, M., Park, P.W., Reizes, O., Fitzgerald, M.L., Lincecum, J., Zako, M., 1999. Functions of cell surface heparan sulfate proteoglycans. Annu. Rev. Biochem. 68, 729–777.

Bink, R.J., Habuchi, H., Lele, Z., Dolk, E., Joore, J., Rauch, G.J., Geisler, R., Wilson, S.W., den Hertog, J., Kimata, K., Zivkovic, D., 2003. Heparan sulfate 6-*O*-sulfotransferase is essential for muscle development in zebrafish. J. Biol. Chem. 278, 31118–31127.

Blackhall, F.H., Merry, C.L., Lyon, M., Jayson, G.C., Folkman, J., Javaherian, K., Gallagher, J.T., 2003. Binding of endostatin to endothelial heparan sulphate shows a differential requirement for specific sulphates. Biochem. J. 375, 131–139.

Bullock, S.L., Fletcher, J.M., Beddington, R.S., Wilson, V.A., 1998. Renal agenesis in mice homozygous for a gene trap mutation in the gene encoding heparan sulfate 2-sulfotransferase. Genes Dev. 12, 1894–1906.

Bulow, H.E., Hobert, O., 2004. Differential sulfations and epimerization define heparan sulfate specificity in nervous system development. Neuron 41, 723–736.

Carmeliet, P., 2000. Mechanisms of angiogenesis and arteriogenesis. Nat. Med. 6, 389–395.

Chen, E., Hermanson, S., Ekker, S.C., 2004. Syndecan-2 is essential for angiogenic sprouting during zebrafish development. Blood 103, 1710–1719.

Esko, J.D., Selleck, S.B., 2002. Order out of chaos: assembly of ligand binding sites in heparan sulfate. Annu. Rev. Biochem. 71, 435–471.

Feyzi, E., Lustig, F., Fager, G., Spillmann, D., Lindahl, U., Salmivirta, M., 1997. Characterization of heparin and heparan sulfate domains binding to the long splice variant of platelet-derived growth factor A chain. J. Biol. Chem. 272, 5518–5524.

Finley, K.R., Davidson, A.E., Ekker, S.C., 2001. Three-color imaging using fluorescent proteins in living zebrafish embryos. Biotechniques 31, 66–70.

Fouquet, B., Weinstein, B.M., Serluca, F.C., Fishman, M.C., 1997. Vessel patterning in the embryo of the zebrafish: guidance by notochord. Dev. Biol. 183, 37–48.

Gibbs, P.D., Schmale, M.C., 2000. GFP as a genetic marker scorable throughout the life cycle of transgenic zebra fish. Mar. Biotechnol. (NY) 2, 107–125.

Habuchi, H., Tanaka, M., Habuchi, O., Yoshida, K., Suzuki, H., Ban, K., Kimata, K., 2000. The occurrence of three isoforms of heparan sulfate 6-*O*-sulfotransferase having different specificities for hexuronic acid adjacent to the targeted *N*-sulfoglucosamine. J. Biol. Chem. 275, 2859–2868.

Habuchi, H., Miyake, G., Nogami, K., Kuroiwa, A., Matsuda, Y., Kusche-Gullberg, M., Habuchi, O., Tanaka, M., Kimata, K., 2003. Biosynthesis of heparan sulphate with diverse structures and functions: two alternatively spliced forms of human heparan sulphate 6-*O*-sulphotransferase-2 having different expression patterns and properties. Biochem. J. 371, 131–142.

Huang, C.C., Lawson, N.D., Weinstein, B.M., Johnson, S.L., 2003. reg6 is required for branching morphogenesis during blood vessel regeneration in zebrafish caudal fins. Dev. Biol. 264, 263–274.

Hyatt, T.M., Ekker, S.C., 1999. Vectors and techniques for ectopic gene expression in zebrafish. Methods Cell Biol. 59, 117–126.

Isogai, S., Horiguchi, M., Weinstein, B.M., 2001. The vascular anatomy of the developing zebrafish: an atlas of embryonic and early larval development. Dev. Biol. 230, 278–301.

Izvolsky, K.I., Shoykhet, D., Yang, Y., Yu, Q., Nugent, M.A., Cardoso, W.V., 2003. Heparan sulfate–FGF10 interactions during lung morphogenesis. Dev. Biol. 258, 185–200.

Jemth, P., Smeds, E., Do, A.T., Habuchi, H., Kimata, K., Lindahl, U.,

Kusche-Gullberg, M., 2003. Oligosaccharide library-based assessment of heparan sulfate 6-*O*-sulfotransferase substrate specificity. J. Biol. Chem. 278, 24371–24376.

Jowett, T., 1999. Analysis of protein and gene expression. Methods Cell Biol. 59, 63–85.

Kamimura, K., Fujise, M., Villa, F., Izumi, S., Habuchi, H., Kimata, K., Nakato, H., 2001. *Drosophila* heparan sulfate 6-*O*-sulfotransferase (dHS6ST) gene. Structure, expression, and function in the formation of the tracheal system. J. Biol. Chem. 276, 17014–17021.

Kimmel, C.B., Ballard, W.W., Kimmel, S.R., Ullmann, B., Schilling, T.F., 1995. Stages of embryonic development of the zebrafish. Dev. Dyn. 203, 253–310.

Lawson, N.D., Weinstein, B.M., 2002. In vivo imaging of embryonic vascular development using transgenic zebrafish. Dev. Biol. 248, 307–318.

Lundin, L., Larsson, H., Kreuger, J., Kanda, S., Lindahl, U., Salmivirta, M., Claesson-Welsh, L., 2000. Selectively desulfated heparin inhibits fibroblast growth factor-induced mitogenicity and angiogenesis. J. Biol. Chem. 275, 24653–24660.

Lyons, M.S., Bell, B., Stainier, D., Peters, K.G., 1998. Isolation of the zebrafish homologues for the tie-1 and tie-2 endothelium-specific receptor tyrosine kinases. Dev. Dyn. 212, 133–140.

Nakato, H., Kimata, K., 2002. Heparan sulfate fine structure and specificity of proteoglycan functions. Biochim. Biophys. Acta 1573, 312–318.

Nasevicius, A., Ekker, S.C., 2000. Effective targeted gene 'knockdown' in zebrafish. Nat. Genet. 26, 216–220.

Nasevicius, A., Larson, J., Ekker, S.C., 2000. Distinct requirements for zebrafish angiogenesis revealed by a VEGF-A morphant. Comp. Funct. Genomics 17, 294–301.

Ono, K., Hattori, H., Takeshita, S., Kurita, A., Ishihara, M., 1999. Structural features in heparin that interact with VEGF165 and modulate its biological activity. Glycobiology 9, 705–711.

Ostrovsky, O., Berman, B., Gallagher, J., Mulloy, B., Fernig, D.G., Delehedde, M., Ron, D., 2002. Differential effects of heparin saccharides on the formation of specific fibroblast growth factor (FGF) and FGF receptor complexes. J. Biol. Chem. 277, 2444–2453.

Parthasarathy, N., Goldberg, I.J., Sivaram, P., Mulloy, B., Flory, D.M., Wagner, W.D., 1994. Oligosaccharide sequences of endothelial cell surface heparan sulfate proteoglycan with affinity for lipoprotein lipase. J. Biol. Chem. 269, 22391–22396.

Perrimon, N., Bernfield, M., 2000. Specificities of heparan sulphate proteoglycans in developmental processes. Nature 404, 725–728.

Pye, D.A., Vives, R.R., Turnbull, J.E., Hyde, P., Gallagher, J.T., 1998. Heparan sulfate oligosaccharides require 6-*O*-sulfation for promotion of basic fibroblast growth factor mitogenic activity. J. Biol. Chem. 273, 22936–22942.

Rapraeger, A.C., 2001. Molecular interactions of syndecans during development. Semin. Cell Dev. Biol. 12, 107–116.

Roman, B.L., Weinstein, B.M., 2000. Building the vertebrate vasculature: research is going swimmingly. Bioessays 22, 882–893.

Rosenberg, R.D., Shworak, N.W., Liu, J., Schwartz, J.J., Zhang, L., 1997. Heparan sulfate proteoglycans of the cardiovascular system. Specific structures emerge but how is synthesis regulated? J. Clin. Invest. 100, S67–S75.

Ruhrberg, C., Gerhardt, H., Golding, M., Watson, R., Ioannidou, S., Fujisawa, H., Betsholtz, C., Shima, D.T., 2002. Spatially restricted patterning cues provided by heparin-binding VEGF-A control blood vessel branching morphogenesis. Genes Dev. 16, 2684–2698.

Smeds, E., Habuchi, H., Do, A.T., Hjertson, E., Grundberg, H., Kimata, K., Lindahl, U., Kusche-Gullberg, M., 2003. Substrate specificities of mouse heparan sulphate glucosaminyl 6-*O*-sulphotransferases. Biochem. J. 372, 371–380.

Thompson, J.D., Higgins, D.G., Gibson, T.J., 1994. CLUSTAL W: improving the sensitivity of progressive multiple sequence alignment through sequence weighting, position-specific gap penalties and weight matrix choice. Nucleic Acids Res. 22, 4673–4680.

Toyoda, H., Kinoshita-Toyoda, A., Fox, B., Selleck, S.B., 2000. Structural analysis of glycosaminoglycans in animals bearing mutations in sugarless, sulfateless, and tout-velu. *Drosophila* homologues of vertebrate genes encoding glycosaminoglycan biosynthetic enzymes. J. Biol. Chem. 275, 21856–21861.

Weinstein, B.M., 2002. Plumbing the mysteries of vascular development using the zebrafish. Semin. Cell Dev. Biol. 13, 515–522.

Zhang, L., Beeler, D.L., Lawrence, R., Lech, M., Liu, J., Davis, J.C., Shriver, Z., Sasisekharan, R., Rosenberg, R.D., 2001. 6-*O*-sulfotransferase-1 represents a critical enzyme in the anticoagulant heparan sulfate biosynthetic pathway. J. Biol. Chem. 276, 42311–42321.